N. P. Kovalenko, Y. P. Krasny, U. Krey

Physics of Amorphous Metals

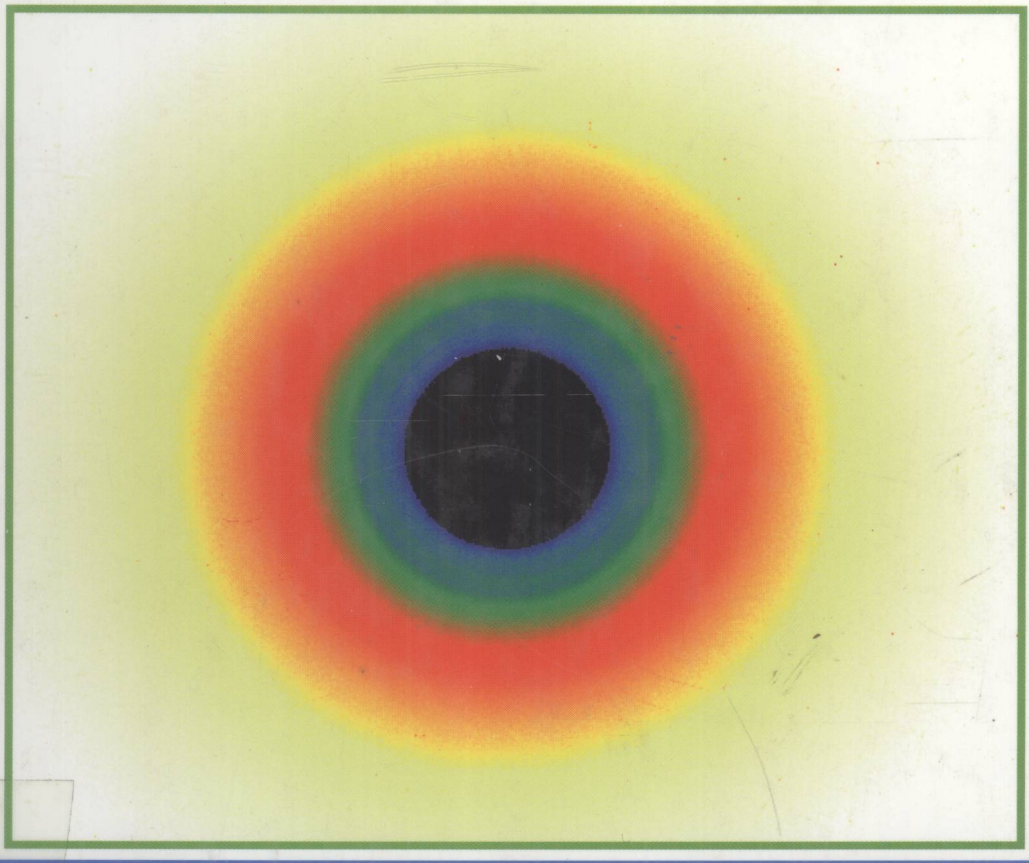

WILEY-VCH

N. P. Kovalenko, Yu. P. Krasny, U. Krey

Physics of Amorphous Metals

WILEY-VCH

Berlin – Weinheim – New York – Chichester – Brisbane – Singapore – Toronto

The Authors of this Volume

Prof. Dr. N. P. Kovalenko
Physics Department
Odessa State University
Ukraine
e-mail: npk@paco.net

Prof. Dr. Yu. P. Krasny
Mathematics Department
University of Opole
Poland
e-mail: krasnyj@math.uni.opole.pl

Prof. Dr. U. Krey
Physics Department II
University of Regensburg
Germany
e-mail: uwe.krey@physik.uni-regensburg.de

Library of Congress Card No.: applied for

A catalogue record for this book is available from the British Library.

Die Deutsche Bibliothek –
CIP Cataloguing-in-Publication-Data
A catalogue record for this publication is available from Die Deutsche Bibliothek.

printed in the
Federal Republic of Germany
printed on acid-free paper

Composition K+V Fotosatz GmbH, Beerfelden, Germany
Printing Strauss Offsetdruck GmbH, Mörlenbach, Germany
Binding J. Schäffer GmbH & Co. KG, Grünstadt, Germany

ISBN 3-527-40315-9

N. P. Kovalenko, Yu. P. Krasny, U. Krey
Physics of Amorphous Metals

Preface

This book deals with amorphous metals, which are systems that nature does not form very often, but which have interesting properties. Usually, metals are polycrystalline or even single-crystalline, i.e. if one starts at high temperatures in the liquid state with one metallic compound only and reduces the temperature slowly below the melting point, there will be *crystallization*. But it has been found experimentally that in cases where the melt is an *alloy* of either (i) two or more metallic compounds, e.g. Cu and Zr, or Mg and Ca, or (ii) of one or more metallic compounds, e.g. 80% Fe, plus one or more so-called *glass formers* such as B, P, Si, C or other so-called *metalloids*, then a sufficiently rapid quench from the temperature of the liquid state to much lower temperatures, which may be in the region of room temperature, typically leads to so-called *amorphous metals*, with a metastable structure of very long lifetime – months, years or decades. These amorphous metals are characterized at least approximately by the fixed 'glassy' structure of a metallic liquid, frozen from just above the melting temperature. Therefore, amorphous metals are also called 'glassy metals', 'metallic glasses' or 'metglasses', and should be distinguished from amorphous semiconductors, e.g. amorphous Si or amorphous Ge, not only because 'metglasses' behave as metals and are often magnetic or even supraconducting, but also because of their different structure: usually, metglasses have a very high coordination number of ≈ 12, as densely packed crystalline metals as Ni, Cu or Co would have, although in those crystalline systems the density of the systems is still higher (typically 14%, see below). In contrast, amorphous Si or Ge are only tetrahedrally coordinated (i.e. the coordination number is only 4), which is of course closely related to their different 'semiconducting' behavior.

The book is centered on the theoretical description, understanding and derivation of the properties of glassy metals. However, advantages and disadvantages of the systems with respect to applications will become clear. Concerning these points one should note that the systems are not simply typical *metals*, but due to the structural properties their metallic resistivity is roughly one or two orders of magnitude higher than that of the typical crystalline counterparts, namely of the same order of magnitude as in the liquid state just above the melting point. At the same time, amorphous metals with Fe, Co and Ni are usually *magnetic* and, in connection with the high resistivity, the material is interesting for voltage trans-

formers, because of their lower electrical losses compared with crystalline Fe–Si transformer material. Thirdly, it is advantageous that the typical pinning centers for magnetic domain walls of crystalline metallic magnets, namely dislocations and grain boundaries, are missing (although a continuous distribution of sources of internal stresses also exists in the amorphous metals). This is the reason for the *extremely soft-magnetic* properties of some of the glassy magnetic materials prepared by industry, which are used for shielding external magnetic fields very efficiently.

However, the applications of the systems are not at the center of this book, which instead stresses the theoretical description of the relevant properties, as already mentioned. This description introduces the relevant theoretical techniques in a self-consistent way, and therein it goes beyond the introductory level. However, we try to keep the applications in mind, whenever possible, and mention the advantageous and disadvantageous properties. Furthermore, although our book emphasizes the *analytical* methods in the theory of amorphous systems and goes as far as to the Eliashberg and Nambu-Gorkov equations in the theory of amorphous superconductivity, we also discuss some of the more recent *numerical* work, i.e. computer simulation methods based on the so-called 'molecular dynamics' and similar techniques, and draw qualitative and semiquantitative conclusions which may be useful not only for the theorist.

Odessa/Opole/Regensburg, January 2001

N. P. Kovalenko
Yu. P. Krasny
U. Krey

Contents

1
On the Structure of Amorphous Metals

1.1
Introduction: Preparation of Amorphous Metals, and Simple Models

Most solids exist in the crystal state. However, at room temperature, there are also *amorphous solids* of essentially two kinds: (i) semiconducting systems, which usually exist as tetrahedrally coordinated networks, and (ii) amorphous *metallic* alloys, which appear in a state that is essentially similar to a frozen picture of a dense metallic liquid composed of at least two different alloy components. (Pure metals apparently do not form a stable or metastable amorphous state, except as films on very cold substrates, e.g. at He temperatures and apparently only with small amounts of impurities (Felsch, 1969, 1970a,b; Leung and Wright, 1974).)

Systems of type (i), e.g. amorphous Si or amorphous Ge, are not the focus of this book. Instead, we concentrate on systems of type (ii), which are often called 'glassy metals', metallic glasses ('metglasses'), or 'amorphous metals'. There are a vast number of such systems, which can be:

(a) composed of at least two different metals, e.g. amorphous $Cu_{1-x}Zr_x$ alloys, which can be prepared in a vast concentration range from $x \approx 0.35$ to $x \approx 0.75$ (or hydrogenated $Fe_{1-x}Zr_xH_y$ or $Mg_{1-x}Ca_x$ alloys, and many other species), or

(b) composed of at least one metallic and one non-metallic 'metalloid' compound, as e.g. amorphous $Fe_{1-x}B_x$, which exists in the composition range between $x=0.15$ and 0.33. These systems are stable in the amorphous state at room temperature, or at least metastable, with lifetimes of up to years or decades, and they can be prepared in different ways.

Some preparation methods are mentioned here, namely

- the so-called 'splat-cooling' technique, in which an 'anvil' with a droplet of the melt on it is hit with a kind of piston – the droplet is quenched immediately to a flat amorphous film;
- the so-called 'melt spinning' method, which is generally applicable to industrial and technical mass production, but is also commonly used in research institutes. The melt is continuously produced by induction heating and dropped in a continuous flow onto a rotating Cu wheel of typically 1 m diameter, such that a continuous ribbon of the amorphous metal is tangentially ejected from the

wheel with a high velocity of typically 2 m/s. The thickness of the ribbons produced in this way is typically 50 μm, and they are up to 2 cm wide;

- the so-called 'solid-state reaction' technique, in which after having produced powders of the alloy components by milling techniques, one can even prepare bulk amorphous metals (Samwer *et al.*, 1994). This technique has apparently not yet found widespread technical applications, whereas the *amorphous magnetic ribbons* produced by melt spinning are actually used for the mass production of active and passive magnetic sensor materials (Hilzinger, 1990).

Other techniques that also deserve mention are the methods of *sputtering* and the method of *laser glazing*.

In addition, large-scale applications of amorphous material, which would have led to a replacement of the conventional FeSi transformer magnets, looked promising in the 1980s, but to date the conventional systems have won the economic competition. In fact, in addition to the difficulty of preparing bulk amorphous metals directly, one of their main shortcomings is the *'aging'* phenomenon, i.e. the fact that the material properties of amorphous metals may deteriorate significantly after cycle times of typically several months or years. As a consequence, the ultra-soft magnetic properties of the shielding material can only be kept for long periods of time if the system is treated very cautiously, both thermally, magnetically and mechanically.

Now let us consider the stability of the amorphous state and questions of model formation. Two of the important physical questions related to these problems concern the 'glass forming ability', and the stability against crystallization. As already mentioned, and as is also known from the conventional non-metallic window glasses, the amorphous state is typically only metastable, and we observe the above-mentioned aging properties. These are of course preparation-dependent, and certain 'annealing procedures', which usually follow the production process, are essential for the quality and stability of industrial products (Hilzinger, 1990). The question therefore naturally arises as to when and why amorphous systems are formed at all.

There are various theoretical aspects to this question, which are intimately related to the problem of modeling the atomic structure of amorphous metals. For example:

(i) the role of deep eutectics

For liquid alloys at a given temperature there exists usually a so-called *miscibility gap*, i.e. a range Δx of concentrations, where the liquid alloy $A_{1-x}B_x$ coexists with separate A resp. B liquids. Considering liquid–vapor phase transitions as an analogon to the demixing transition, the analogon to the miscibility gap is the coexistence region between a single-component liquid and the corresponding vapor phase, and the density range of coexistence, $\Delta\rho$, plays a role corresponding to that of Δx. Outside the miscibility gap, a liquid alloy phase is not thermodynamically stable. With decreasing temperature of the melt, Δx becomes gradually smaller and smaller, until at a low, so-called 'eutectic temperature', which may approach

the range of room temperature, a single so-called *eutectic composition* x_t remains. In this eutectic concentration region the glass-forming ability after a rapid quench is particularly high, which seems natural, but is not easy to formulate quantitatively.

(ii) hard-sphere models

There are also '*steric*' aspects (i.e. in contrast to energetic ones) that favor amorphization. One of the first models to describe amorphous alloys was the so-called *Bernal model*, i.e. a dense random packing of hard spheres (Bernal, 1959, 1960): If we try to compress a large set of hard spheres, i.e. taken from ball bearings, into a box, e.g. 80% of the atoms resembling Fe in its atomic radius, and 20% with a radius corresponding to B, then we usually end up with a metastable state. Finney and coworkers have produced such models by hand (Finney, 1970) and found that the packing fraction $f = N(4\pi r^3/3)/V$ of such models, if we are dealing with fictitious one-component cases, are somewhat lower (typically $\approx 14\%$) than those of crystalline face-centered or hexagonal crystals, namely 0.6366 ± 0.0004 instead of 0.74 (Finney, 1970). Here r is the hard-core radius of the atoms, N the number of balls, and V the volume of the box considered. Furthermore, it has been found that in such models there is a sufficient number of small holes, into which 20% small 'B spheres' would fit. More details will be discussed in the following section.

1.2 The Radial Distribution Function and the Structure Function

A more complete picture of the structure of amorphous systems can only be obtained by the set of averaged n-point correlation functions for $n = 2, 3, 4, \ldots$, namely

$$F_n(\mathbf{R}_1, \mathbf{R}_2, \ldots, \mathbf{R}_n) = \overline{\delta(\mathbf{r}_1 - \mathbf{R}_1)\delta(\mathbf{r}_2 - \mathbf{R}_2)\ldots\delta(\mathbf{r}_n - \mathbf{R}_n)} \tag{1.2.1}$$

Here, the $\mathbf{r}_i$ denote the positions of the n atoms, $\delta(\mathbf{r})$ is Dirac's Delta function and the overbar denotes an average over an ensemble of amorphous systems with the same statistical properties as the considered one. We assume in the following that this ensemble can be obtained by 'self-averaging', i.e. in the so-called *thermodynamic limit* of infinite system size, $V \to \infty$, the system can be divided into infinite blocks, which represent the samples of the ensemble. Thus we also assume *statistical homogeneity* of the system, i.e. the averages and averaged correlation functions considered are assumed to be translationally invariant.

The most important of the averaged correlation functions in Eq. (1.2.1) is the so-called *Radial Distribution Function* $\rho(\mathbf{r})$, and the so-called *Partial Radial Distributions* $\rho_{\alpha\beta}(\mathbf{r})$ (see below), which can be derived from Eq. (1.2.1) for $r := |\mathbf{r}_1 - \mathbf{r}_2|$ with $n = 2$. These functions appear throughout the following chapters, when the thermodynamics of vibrational, magnetic, electronic and superconducting excitations in amorphous metals are considered, and this is why we emphasise them here.

In fact, $\rho(\mathbf{r})$ and $\rho_{\alpha\beta}(\mathbf{r})$ can most easily be determined for computer models of amorphous systems, just by counting the numbers of atoms of kind β that are at a distance between r and $r + dr$ from a fixed atom of kind α, and averaging over all atoms α, see below. Experimentally, their determination is somewhat more involved and involves diffraction experiments utilizing X-ray diffraction, electron diffraction or neutron diffraction, or combinations thereof. Namely, for the different diffraction sources, the *scattering amplitudes* f_α (see below) are different, such that from the differences of the scattering cross-sections $d\sigma/d\Omega$ obtained by three different experiments we can usually determine the partial radial distribution functions $\rho_{\alpha\beta}(\mathbf{r})$ for binary amorphous alloys, i.e. with $\alpha, \beta = 1, 2$. (With neutron scattering, we can also use amorphous alloys of the same composition, but with different *isotopes* of the compounds considered, because these isotopes sometimes also have very different neutron scattering lengths.)

The description of the diffraction experiments, and their relation to the radial distribution functions, is as follows.

Let a monochromous beam of X-ray photons, or electrons, or neutrons, impinge onto our amorphous sample of volume V and particle number N. The monochromous beam is assumed to have a current-density j_0 $(= dN_0/(dt\ cm^2))$ and an incoming wavevector $\mathbf{k_i} = k\mathbf{e_z}$, where $\lambda = 2\pi/k$ is the wavelength or de Broglie wavelength of the particles and $\mathbf{e_z}$ the direction of the flow (the z-direction without restriction). The particles are scattered elastically, and a counter, which is at a very large distance r from the sample, counts the number N_s of scattered particles with polar scattering angles between θ and $\theta + d\theta$, and azimuthal ones between ϕ and $\phi + d\phi$. The solid angle $d\Omega$ covered by the counter is thus given by $d\Omega = \sin\theta\, d\theta\, d\phi$. From the number of counts per second, dN_s/dt, by the counter, we can thus determine *experimentally* the so-called differential cross-section:

$$(d\sigma/d\Omega) = (dN_s/dt)/(j_0 d\Omega) \tag{1.2.2}$$

Theoretically, $d\sigma/d\Omega$ is given by the following expression:

$$(d\sigma/d\Omega)(\mathbf{q}) = \overline{|\sum_{i=1}^{N} f_i \exp[i\mathbf{q}(\mathbf{r} - \mathbf{r}_i)]|^2} \tag{1.2.3}$$

Here, as already mentioned, $\mathbf{r}$ is the position of the counter and $\mathbf{r}_i$ are the positions of the scattering atoms in the amorphous sample; $|\mathbf{r}|$ is always $>> |\mathbf{r}_i|$, i.e. the center of mass of the amorphous sample can be taken as the origin. The vector $\mathbf{q} = \mathbf{k}_f - \mathbf{k}_i$ is the difference between the wavenumbers of the scattered particle before and after the scattering. Finally, for the magnitude we have $|\mathbf{q}| = (4\pi/\lambda)\sin(\theta/2)$, and the f_i are the complex scattering amplitudes.

Now, by evaluation of Eq. (1.2.3), it follows that for an amorphous alloy with $\alpha = 1, 2, .., n$ different alloy components:

$$(d\sigma/d\Omega) = N \sum_{\alpha,\beta=1}^{n} c_\alpha c_\beta f_\alpha^* f_\beta \int d^3r \exp(i\mathbf{q}\,\mathbf{r}) \rho_{\alpha\beta}(r) \tag{1.2.4}$$

Here the product $c_\beta 4\pi r^2 dr\rho_{\alpha\beta}(r)$ is the expectation value of the number of β atoms that have a distance between r and $r + dr$ from a given α atom. Thus, for $r \to \infty$, $\rho_{\alpha\beta}(r)$ converges to $\rho_0 := (N/V) =: 1/v_0$, i.e. the reciprocal of the specific volume, independent from α and β, and for the Fourier transform of $\rho_{\alpha\beta}(r)$, we obtain

$$S_{\alpha\beta}(q) = \int d^3r \exp(i\mathbf{q} \cdot \mathbf{r})\rho_{\alpha\beta}(r) = [(2\pi)^3/v_0]\delta(\mathbf{q}) + a_{\alpha\beta}(q) \tag{1.2.5}$$

Here $a_{\alpha\beta}(q)$ is the so-called *Partial Structure Function*, which is often used in the following chapters. According to Eq. (1.2.4) we thus have

$$(d\sigma/d\Omega) = N\Sigma_{\alpha\beta}c_\alpha c_\beta f_\alpha^* f_\beta S_{\alpha\beta}(q) \tag{1.2.6}$$

In this way, from the experiments, $S_{\alpha\beta}(q)$ and thus $\rho_{\alpha\beta}(r)$ can be determined. By the spherical symmetry of both quantities, we can reduce the necessary integrations to one-dimensional ones from 0 to ∞, namely

$$a_{\alpha\beta}(q) = 4\pi \int_0^\infty r^2 dr[\sin(qr)/(qr)][\rho_{\alpha\beta}(r) - \rho_0] \tag{1.2.7}$$

$$\rho_{\alpha\beta}(r) = \rho_0 + (2\pi^2)^{-1} \int_0^\infty q^2 dq[\sin(qr)/(qr)]a_{\alpha\beta}(q) \tag{1.2.8}$$

As can be seen from Eq. (1.2.8), it is sometimes useful to plot the following 'reduced radial distribution' $G_{\alpha\beta}(r)$, which is used in some of the following figures:

$$G_{\alpha\beta}(r) := 4\pi r[\rho_{\alpha\beta}(r)\rho_0] \tag{1.2.9}$$

which for $q \neq 0$ is related to $a_{\alpha\beta}(q)$ by

$$a_{\alpha\beta}(q) = (1/q) \int_0^\infty dr G_{\alpha\beta}(r) \sin(qr) \tag{1.2.10}$$

and

$$G_{\alpha\beta}(r) = (2/\pi) \int_0^\infty dq[qa_{\alpha\beta}(q)] \sin(qr) \tag{1.2.11}$$

Figures 1.2.1, 1.2.2 and 1.2.3 present the partial distribution functions $\rho(r)$ and the structure functions $S(q)$, which von Heimendahl (1979) calculated from a computer simulation for the structure of a two-component metallic glass, namely for $Mg_{70}Zn_{30}$. The calculation produced a 'relaxed hard-core model' of 800 atoms; such models are often more simply called 'soft-core models'. In the calculation,

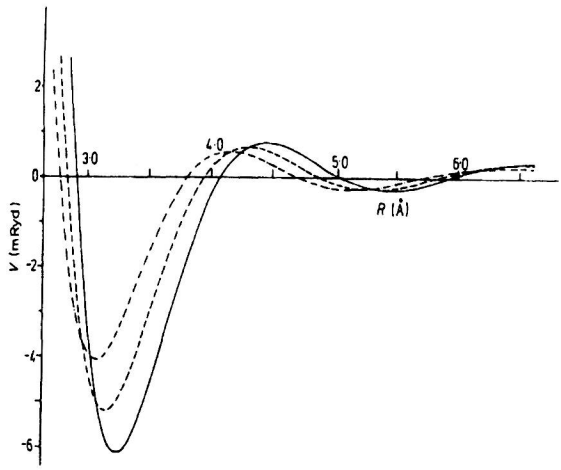

Fig. 1.2.1 The pair potentials used in the computer simulation of von Heimendahl (1979). This simulation produced a 'soft-core model' for $Mg_{70}Zn_{30}$ with 800 atoms in a box with periodic boundary conditions. In the calculation, three effective pair potentials were used, calculated by J. Hafner (Hafner, 1976, 1977a,b) from the general non-local 'pseudopotential theory' described in Chapter 2. In this figure, the 'deepest', 'second deepest' and 'most shallow' lines, respectively, represent the pair potentials for MgMg, Mg-Zn and Zn-Zn

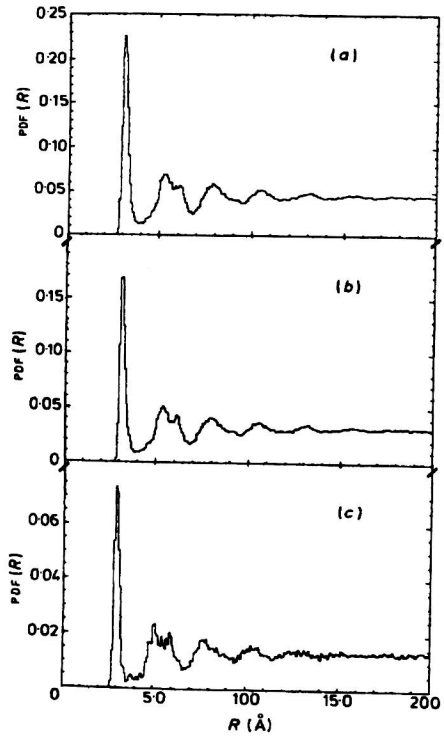

Fig. 1.2.2 The total 'radial distribution function' $\rho(r)$ for the amorphous model system $Mg_{70}Zn_{30}$ according to the computer simulation of von Heimendahl (1979). Parts b and c represent the partial radial distribution functions corresponding to the Mg-Mg and Zn-Zn correlations respectively

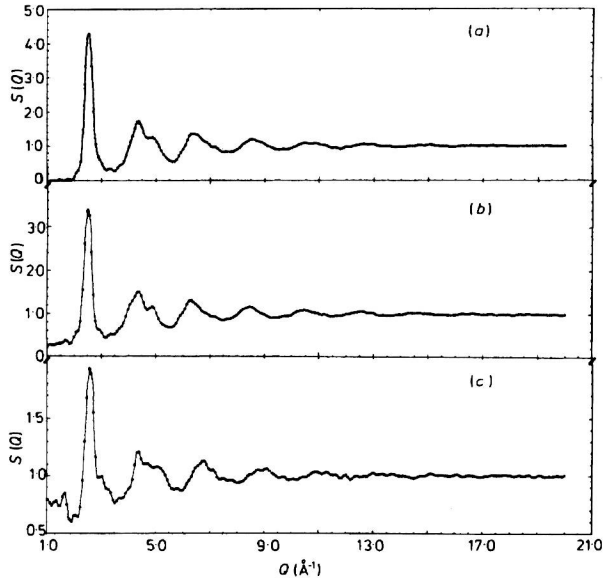

Fig. 1.2.3 The corresponding 'structure function' $S(q)$ to Fig. 1.20.2 for the amorphous model system $Mg_{70}Zn_{30}$ according to the computer simulation of von Heimendahl (1979). Parts b and c represent the partial radial distribution functions and partial structure functions corresponding to the Mg-Mg and Zn-Zn correlations respectively

three effective pair potentials were used, calculated by J. Hafner (Hafner, 1976, 1977a,b) from the general 'non-local pseudopotential theory' described in Chapter 2. Figure 1.2.1 shows these pair potentials: in this figure, the 'deepest', 'second deepest' and 'most shallow' lines, respectively, present the pair potentials for Mg-Mg, Mg-Zn and Zn-Zn. Figure 1.2.2 depicts the total radial distribution (part a) and the partial distribution functions $\rho_{\text{Mg-Mg}}(r)$, part b, and $\rho_{\text{Zn-Zn}}(r)$, part c. Finally Fig. 1.2.3 (a, b, c) shows the corresponding 'structure functions' $a_{\alpha\beta}(q)$ (= $S_{\alpha\beta}(q)$ for $q \neq 0$).

1.3 Structural Models of Glassy Metals

As already mentioned in Section 1.1, there are many models constructed so as to yield a sufficient description of metallic glasses. The earliest models were in fact constructed 'by hand', i.e. the Finney model (Finney, 1970), one of the most prominent DRPHS models (DRPHS = *D*ense *R*andom *P*ackings of *H*ard *S*pheres).

Figure 1.3.1 shows the total 'reduced radial distribution function' $G(r)$ for Finney's hard-sphere model, compared with experimental results.

Here the first pronounced peak corresponding to the nearest-neighbor shell and the hard-core condition is most clearly visible, as is the following pronounced

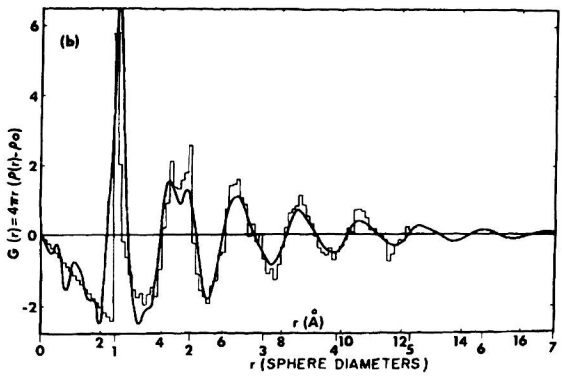

Fig. 1.3.1 Comparison of the reduced radial distribution function $G(r)$ obtained from Finney's original ball bearing model (the histogram) with experiments for amorphous $Ni_{76}P_{24}$ (Cargill, 1975, p. 304)

minimum, followed by a second, less pronounced 'split' maximum, corresponding to the shell of second- and third-nearest neighbors. However, the shortcomings of the DRPHS model can also be clearly seen by the comparison with experiment. Namely, in the DRPHS model, because of the hard-core condition, there are no Fe atoms with distances less than $2r_0$, where r_0 is the hard-core radius corresponding to Fe, namely $r_0 = 2.86$ Å, whereas in reality (i.e. for the solid line in Fig. 1.3.1, and also in Fig. 1.3.2) the first peak, corresponding to the shell of 'nearest neighbors', although being quite pronounced, is clearly somewhat 'smeared' over a small but finite range, and also the two smaller peaks in the following shell corresponding to second- and third-nearest neighbors are different in reality: in the DRPHS model, the second of these two peaks is clearly more pronounced, which is the opposite of reality (see Fig. 1.3.2).

Furthermore, in the liquid state of metallic glasses, as opposed to the amorphous one, there is no splitting at all (Fig. 1.3.3), but otherwise the radial distributions for liquid metals just above the melting point are quite similar to those of the amorphous state, which justifies the 'frozen liquid' picture mentioned above.

These observations give a clear hint that hard-core models are oversimplified and should be used with care. At least the positions of the atoms in such models should be energetically *'relaxed'* in realistic inter-ionic potentials, e.g. the self-consistent pseudopotentials discussed in the next chapter. The improved models based on such procedures could be termed DRPSS models (i.e. Dense Random Packings of 'Soft Spheres'), or simply soft-sphere models.

For liquids there is a well-known analytical treatment of the radial distribution function in hard-sphere approximation, the *Percus-Yevick* approximation (Percus and Yevick, 1958). We do not describe this here, because there are several comprehensive reviews on it available (e.g. Kovalenko and Fisher, 1973). Results from this approximation are shown in Fig. 1.3.4, which should be compared with those of Fig. 1.3.3.

Because the agreement is reasonable, even with the results for the amorphous metals in Fig. 1.3.2, and because there are further approximations made in the

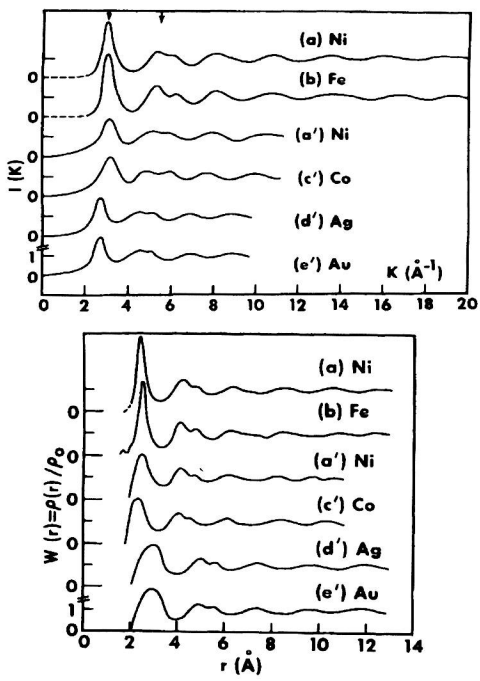

Fig. 1.3.2 Interference function $I(k)$, $\equiv S(q)$ in the text (upper part), and radial distribution function $W(r)=\rho(r)/\rho_0(r)$ (lower part) for amorphous films of different metals, after Cargill (1975), p. 262. The results for amorphous Ni and Fe (a,b) are taken from Ichikawa (1973), and for the amorphous films of Ni, Co, Ag and Au (a',c',d',e') from Davies and Grundy (1971, 1972)

analytical treatment of the excitations discussed in later chapters, the 'liquid-like' Percus-Yevick radial distribution function will be used frequently below.

As just mentioned, to obtain more realistic models of metallic glasses as a prerequisite for calculations of vibrational, spin, electronic or superconducting excita-

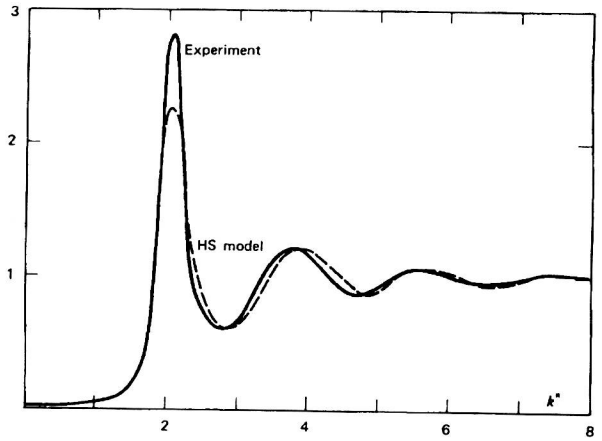

Fig. 1.3.3 The 'structure function' $S(q)$ of liquid Na is compared with results from a 'molecular dynamics' simulation (hard-sphere model) corresponding to high densities, i.e. with a filling factor of the hard spheres of $\eta = 45\%$ of the volume (after Balescu, 1975, p. 288)